

# Measuring photon correlations simultaneously in time and frequency

Blanca Silva,<sup>1,2</sup> Alejandro González Tudela,<sup>3</sup> Carlos Sánchez Muñoz,<sup>1</sup> Dario Ballarini,<sup>2</sup> Milena de Giorgi,<sup>2</sup> Giuseppe Gigli,<sup>2</sup> Kenneth W. West,<sup>4</sup> Loren Pfeiffer,<sup>4</sup> Elena del Valle,<sup>1</sup> Daniele Sanvitto,<sup>2</sup> and Fabrice P. Laussy<sup>1,5</sup>

<sup>1</sup>*Departamento de Física Teórica de la Materia Condensada,  
Universidad Autónoma de Madrid, E-28049 Madrid, Spain*

<sup>2</sup>*NNL, Istituto Nanoscienze – CNR, 73100 Lecce, Italy*

<sup>3</sup>*Max-Planck Institut für Quantenoptik, 85748 Garching, Germany*

<sup>4</sup>*Department of Electrical Engineering, Princeton University, Princeton, New Jersey 08544, USA*

<sup>5</sup>*Russian Quantum Center, Novaya 100, 143025 Skolkovo, Moscow Region, Russia\**

(Dated: March 21, 2022)

The two-photon spectrum—that retains the energy as well as the time of detection in two-photon correlation measurements—is obtained in closed-form for an arbitrary initial quantum state and measured experimentally from the spontaneous emission of a polariton condensate. Two-photon colored bunching and antibunching are observed depending on the frequency of detection, as a manifestation of Bose statistics in systems lacking a common phase reference. These results validate and extend the conventional Glauber’s theory of photon correlations and open the page of two-photon correlation spectroscopy.

PACS numbers: 42.50.-p, 42.50.Ar, 67.10.-j, 03.65.Yz, 03.75.Nt

The science of photon correlations—quantum optics—started with the seminal observation by Hanbury Brown and Twiss that photons from thermal light exhibit bunching in their arrival time.<sup>1</sup> This led to Glauber’s Nobel prize for the theory of optical coherence in a quantum setting.<sup>2</sup> The standard approach to quantify photon correlations since then is through correlators of the type:

$$g^{(2)}(t, \tau) = \frac{\langle a^\dagger(t) a^\dagger(t + \tau) a(t + \tau) a(t) \rangle}{\langle a^\dagger(t) a(t) \rangle \langle a^\dagger(t + \tau) a(t + \tau) \rangle} \quad (1)$$

with  $a(t)$  the light field annihilation operator at time  $t$ , and  $\tau$  the time delay between detections. This quantity—the second-order correlation function—describes the statistical distribution between photons in their stream of temporal detection. Other properties of the photons can be included, e.g., their position<sup>1,3</sup> or polarisation,<sup>4</sup> with applications spanning from subatomic interferometry<sup>5</sup> to entangled photon pair generation.<sup>6</sup> Of all the possible additional variables, one is so intertwined with the temporal information as to requalify the meaning of photon correlations: it is the energy of the photon (or, equivalently, its frequency). This is a characterisation of a different type than position or polarisation since time and frequency are conjugate variables. This results in a wider and unifying perspective of photon correlations, that provides as much information as can be retrieved according to quantum mechanics.<sup>7,8</sup> The formal theory of time and frequency resolved correlations, established in the 80s,<sup>7–10</sup> upgrades Eq. (1) to the two-photon frequency correlations:

$$g_\Gamma^{(2)}(\omega_1, T_1; \omega_2, T_2) = \frac{\langle : \mathcal{T} [\prod_{i=1}^2 A_{\omega_i, \Gamma}^\dagger(T_i) A_{\omega_i, \Gamma}(T_i)] : \rangle}{\prod_{i=1}^2 \langle A_{\omega_i, \Gamma}^\dagger(T_i) A_{\omega_i, \Gamma}(T_i) \rangle} \quad (2)$$

where  $A_{\omega_i, \Gamma}(T_i) = \int_{-\infty}^{T_i} e^{i\omega_i t} e^{-\Gamma(T_i-t)/2} a(t) dt$  is the field of frequency component  $\omega_i$  and width  $\Gamma$ , at time  $T_i$ , and  $\mathcal{T}$ , (resp.  $:$ ) refers to time (resp. normal) ordering. Equation (S1) provides the tendency of a correlated detection of one photon of frequency  $\omega_1$  at time  $T_1$  with another photon of frequency  $\omega_2$  at time  $T_2$ . This is an increasingly popular experimental quantity, with already many measurements performed but for fixed sets of frequencies, by inserting filters in the paths of a standard Hanbury Brown–Twiss setup.<sup>11–16</sup> The real measure of its conceptual importance, however, is given when spanning over all possible combinations of frequencies. This gives rise to a so-called “two-photon correlation spectrum” (2PS)<sup>17</sup>. Considering the most important case of coincidences— $\tau = 0$  in Eq. (1) and  $T_1 = T_2$  in Eq. (S1)—one elevates in this way a single number,  $g_0^{(2)} \equiv g^{(2)}(t = 0, \tau = 0)$ , to a full landscape  $g_\Gamma^{(2)}(\omega_1, \omega_2; \tau = 0)$  of correlations. It is only recently that such landscapes could be computed without approximations thanks to a new theory of photo-detection.<sup>18</sup>

\*Electronic address: fabrice.laussy@gmail.com

The 2PS characterises the full two-photon dynamics of the system, that is, including also emission and detection. This is in stark contrast with Eq. (1) that, at  $\tau = 0$ , only requires the quantum state specified by its density matrix  $\rho(t)$  with no further information on the underlying Hamiltonian. On the other hand, if one wants to keep track of the frequency information, there is the need to specify which dynamics is bringing the photons from the state towards the detectors that will correlate them. The fact that such fundamental issues are required to compute the 2PS indicates that it is more physical than the conventional  $g_0^{(2)}$ . The most basic process to bring a photon from the quantum state toward a detector is spontaneous emission, followed by free propagation toward the detector that performs the frequency-filtering and correlation. In preparation of a point to be discussed shortly, we also include the other fundamental type of dissipation for the density matrix, dephasing, which also affects the phase (off-diagonal elements) while the radiative lifetime affects the populations only (diagonal elements).<sup>39</sup> This provides us with the master equation  $\partial_t \rho = [\frac{\gamma_a}{2} \mathcal{L}_a + \frac{\gamma_\phi}{2} \mathcal{L}_{a^\dagger a}] \rho$  with  $\gamma_a$  and  $\gamma_\phi$  the radiative and dephasing rates, respectively, in the Lindblad form  $\mathcal{L}$ . This equation can be solved exactly (Eq. (4) in Methods), from which one can compute observables such as  $n(t) = \langle a^\dagger a \rangle(t) = n(0) \exp(-\gamma_a t)$ , as expected on physical grounds despite the complicated form of the general solution. For the main quantity of interest in our discussion, Eq. (1), one finds that the photon statistics is constant in both real and autocorrelation time:  $g^{(2)}(t, \tau) = g^{(2)}(0, 0)$ . Because this result may appear either trivial or pathological, it has received, to the best of our knowledge, no attention in the literature. When considering frequency correlations, however, since the time dynamics is required in the calculation even for coincidences, such properties take on a physical meaning. This result also justifies the validity of Glauber's  $g_0^{(2)}$  even though photon emission and detection is disregarded. Indeed, we demonstrate (the theoretical details are given in the Supplementary Material) that in the case of spontaneous emission, Glauber's theory gets upgraded by frequency correlations to the following form:

$$g_\Gamma^{(2)}(\omega_1, \omega_2) = g_0^{(2)} \mathcal{F}_\Gamma(\omega_1, \omega_2), \quad (3)$$

with  $\mathcal{F}_\Gamma(\omega_1, \omega_2)$  a *boson form factor*, which is independent of the quantum state  $\rho$  in which the system is prepared, and depends only on the dynamics of emission and detection. The analytical expression for  $\mathcal{F}_\Gamma$  is given in the Methods section, Eq. (5). This quantity is the missing link between Glauber's theory that pertains to the quantum state and photo-detection theory that connects it to the experiment. If averaging over frequencies, the conventional  $g_0^{(2)}$  is recovered.

To prove this new general form of Glauber's theory, in this work we demonstrate experimentally such a full mapping of time- and frequency-resolved photon correlations for the fundamental dynamics that mixes decoherence and decay in a bosonic system. The measurement is made with a new setup based on a streak camera under continuous wave (CW) excitation, from the spontaneous emission of a steady state condensate of polaritons, i.e., strongly-coupled light-matter bosonic particles in a semiconductor microcavity.<sup>19</sup> We use the photon stream coming from a polariton condensate, not only for the intrinsic importance of Bose–Einstein condensation, but also because it provides a tunable and convenient realisation in the steady state of popular quantum states, from thermal to coherent, for which the conventional  $g_0^{(2)}$  is well-known. The spectral broadening of polaritons as well as their intensity make them convenient to undertake such a demanding measurement. Both the principle and the technique are, however, general and should allow, with optimisation, to revisit systematically all of quantum optics, starting with quantum sources. The setup is sketched in Fig. 1(a) and is detailed in the Methods section. To summarise the basics: light is dispersed by a monochromator and is directed into a streak camera that operates at the single-photon level, as has already been demonstrated with standard photon correlations in time domain only, under pulsed excitation.<sup>20</sup> The sweeping in time and dispersion in energy allow the simultaneous recording of both the time and frequency of each detected photon in successive frames that are post-processed to calculate intensity correlations. A scheme of the emitter is shown in Fig. 1(b): polaritons condense into the ground state from a reservoir of high energy polaritons injected by a CW off-resonant laser. There are constant losses, chiefly through the cavity mirror, which allow to study the steady-state correlations. The reservoir relaxation into the condensate is typically phonon-mediated and establishes a nontrivial quantum coherence between the two systems,<sup>21</sup> that is responsible for the spontaneous coherence buildup.<sup>22</sup> The experiment is performed by recording several hundred thousands frames which detect the photon time arrival, energy resolved, during a time span of 200 ns (see Methods for details). There is no phase locking between the successive frames, corresponding to  $\gamma_\phi \neq 0$ . Interestingly, when  $\gamma_\phi = 0$ , i.e., considering the decay (emission) as the only dynamics of a quantum state, one obtains  $\mathcal{F}_\Gamma(\omega_1, \omega_2) = 1$  and Glauber's theory is complete even when discriminating in frequency: the detected photon statistics is that calculated with only the density matrix. So, for instance, assuming the case of a Fock state of two polaritons  $|2\rangle$ , left to decay, one would find, regardless of the frequency at which the photons they emitted have been detected, that their correlation is  $1/2$ . This is, at first sight, a surprising result in the light of two-photon correlation spectra computed in a steady state,<sup>18</sup> because two photons emitted at the same frequency would be expected to exhibit more photon bunching due to the indistinguishability of Bose particles than two photons from the same system but, from fluctuations in the emission, emitted at different frequencies. The

loophole here is linked to the role of reference frames in quantum mechanics.<sup>23</sup> Like any quantum observable,  $g^{(2)}$  is by essence a statistical quantity. Photon detection is a demolition measurement and to acquire enough signal, the experiment needs to be repeated<sup>24</sup>. While we have included photon detection and emission through decay  $\gamma_a$  by the emitter and absorption  $\Gamma$  by the detector, we have left the state preparation unaddressed by assuming the possibility to prepare a perfect initial condition at exactly  $t = 0$ . This is what allows photons infinitely remote in time to be correlated as well as their resilience to Bose statistics. To take fully into account all that actually happens in the experiment, one should include state preparation as well. The physics that is lost in this omission is the two references frames—that of the emitter on the one hand and of the detector on the other hand—not systematically agreeing on their “zero” of the phase. The lack of a locked phase from experiment to experiment lifts the reference ordering and results in photon indistinguishability effects,<sup>23</sup> namely with tendency of photon bunching when detecting at the same frequency and of antibunching when detecting at diametrically opposed frequencies. Indeed,  $\mathcal{F}_\Gamma$  with  $\gamma_\phi \neq 0$  exhibits a characteristic profile of bunching on the diagonal and antibunching on the antidiagonal. This is shown in Fig. 1c. This is the typical case for most experiments, with no synchronisation of the phase from one event to the next, and affects their overall correlation as specified by  $g_0^{(2)}$ . When considering the corresponding problem for a steady state, as in the case of our experiment, the excitation is explicitly taken into account in the dynamics and photon-correlations always exhibit the expected tendencies for bunching and antibunching with different overlaps in frequency, with no need of an ad-hoc dephasing term. The repetition of the experiment in this case is instead self-consistently included in the model, since a continuous stream of photons is randomly delivered to the detectors, with a corresponding randomization of the phase. The boson form factor is therefore a fundamental quantity that describes boson correlations in their simplest form. We conjecture that fermion correlations would be similar but with an orthogonal profile: antibunching on the diagonal and bunching on the antidiagonal; this question, that could be investigated for instance in transport experiments with electrons,<sup>25</sup> is however outside the scope of this text. The theoretical calculation corresponding to the steady state experiment is shown for photon coincidences ( $\tau = 0$ ) in Fig. 2(a) in a regime close to threshold, where the state is in mixture of a thermal and a coherent state. The predicted 2PS is qualitatively similar to the fundamental structure of spontaneous emission of an initial state, Fig. 1(c), as could be expected since this is essentially what the polariton steady state provides. Nevertheless, its dynamics does not reduce exactly to that case, since the mechanism of coherence buildup results in some quantitative departures.

With the procedure described previously, we are able to obtain  $g_\Gamma^{(2)}(\omega_1, \omega_2; \tau)$  experimentally. In Fig. 2b, we show the experimental 2PS for the polariton condensate at  $\tau = 0$ . An excellent agreement with the theory is obtained, especially for the salient features which are diagonal bunching and antidiagonal antibunching. This is also the first time that a polariton system exhibits, from a macroscopic phase, anticorrelations at the single particle level. These do not correspond to violation of classical inequalities, however, which are typically, and counter-intuitively, associated to bunching instead.<sup>26</sup> The data required prolonged acquisition times in extremely stable conditions to collect millions of events to reconstruct the landscape of photon correlations, and although they have some level of noise, the features are unambiguous. In Fig. 2c, we show the temporal correlations for three points of the  $(\omega_1, \omega_2)$ -space, both for the experiment and the theoretical model. Again, there is an extremely good agreement and a clear evolution of the correlations from bunching ( $g_\Gamma^{(2)}(\omega, \omega; 0) \approx 1.5$  in region 1) to antibunching ( $g_\Gamma^{(2)}(-\omega, \omega; 0) \approx 0.7$  in region 3). Such a two-colour antibunching has been reported before, e.g., from quantum dots in microcavities<sup>12</sup> or from colloidal nanocrystals especially engineered for that purpose.<sup>16</sup> In contrast, our source is not a quantum emitter and its auto-correlation exhibits bunching, thereby providing still another type of correlated photons source. Furthermore, correlations are extracted from within the same peak, rather than from two already distinguishable peaks, and therefore demonstrates frequency-filtering from a single mode rather than two-mode correlations. Another fundamental feature of the theory is that correlations depend on the frequency windows that select which photons are correlated. Smaller windows lead to stronger correlations but, again, at the price of a smaller signal. In Fig. 3, we show the dependence of the 2PS on the size of the frequency windows for a point that features antibunching. When the frequency window is very large,  $\Gamma \gg \gamma_a$ , both the experimental and theoretical  $g^{(2)}(\omega_1, \omega_2; \tau)$  recover as expected the results of standard photon correlations which has always been reported to be larger than 1 for these kinds of systems.<sup>27–29</sup> As the size of the frequency window decreases, the system shows a transition from bunching to antibunching, demonstrating how the statistics of coloured photons can be easily tuned externally. The observation matches again extremely well with the theory.

Bunching of photons is a known feature of spectral filtering from a single peak<sup>30</sup> but it was investigated in a particular context only, namely, of coherent emission from a CW laser, and attributing it to fluctuations, which is too specific and restricted to an inessential aspect of the dynamics. Also, it focused on the main peak rather than reconstructing the full 2PS and missed for that reason the overall picture and therefore the regions of antibunching. We show here instead that both two-color bunching and antibunching are in fact intrinsic features that apply universally to all dynamical evolutions of all bosonic systems as a consequence of their statistical properties in the absence of a common and synchronised phase reference frame. We have not included fluctuations here since they are not needed to explain the findings in an experiment using a single mode laser where we have been very careful to stabilise the

state. However, fluctuations also have a bearing on the discussion and our technique should have applications in the measurement of spectral diffusion when applied to fluctuating systems<sup>14</sup> where it should also allow to win another three orders of magnitude precision. Finally, the 2PS has a nontrivial and non-factorable form of the type of Eq. (S13) whenever there is a richer dynamic of emission than merely spontaneous emission.<sup>17,18</sup> We have already mentioned how the mechanism of condensation indeed results in some small deviation from the spontaneous emission boson form factor. In cases of strongly correlated emission, such as dressing of states which opens channels of emission through virtual processes,<sup>26,31</sup> the 2PS presents strong geometric features, such as antidiagonals or circles of correlations.<sup>17</sup> This provides the full photon correlations inherited from the system dynamics, that are otherwise lost by disregarding the frequencies, resulting in washing out rich landscapes to reduce them to a single, essentially meaningless number, as specified by the standard theory. The most valuable input of the 2PS for practical purposes will be, therefore, in such situations where the exploitation of photon correlations in schemes akin to distillation<sup>32</sup> or Purcell enhancement<sup>31</sup> will be used to power quantum technology. This will rely on more complex structures from strongly correlated states, while we have here addressed the fundamental case of spontaneous emission of a quantum state maintained in a steady state so as to be analogous to an initial condition. We have demonstrated, doing so, that both the concept and technique of colour correlations are sound and ripe to be deployed in a large range of quantum optical systems, with prospects of accessing further classes of quantum correlations<sup>33,34</sup> or optimising those already known<sup>26,32</sup>. Platforms such as superconducting qubits, that have achieved an impressive control of conventional quantum correlations,<sup>35</sup> should be able to extend this technique to unravel the much richer quantum landscapes sculpted in the light field by a two-level system.<sup>17</sup>

## Methods

*Experiments:* The sample is a semiconductor microcavity with high reflective Bragg mirrors and  $3 \times 4$  quantum wells at the antinodes of a  $2\lambda$  cavity. It is pumped at normal incidence and non-resonantly with a single-mode laser at a wavelength of 725.2 nm. Each photon emitted by the lower polariton state is mapped to a pixel in the streak detector with a temporal and spectral resolution of 3.2 ps and 70  $\mu$ eV respectively in a total window of 1536 ps  $\times$  456.7  $\mu$ eV. The correlation landscapes are obtained from correlations between these clicks ( $\approx 1.69$  per sweep in a total of 350 000 frames). We found it important not to use a chopper, that introduces long timescales correlations due to heating and cooling of the sample that result in non-stationarity of the photon statistics, although this is not apparent through single-photon observables such as the intensity. This, of course, limits the range of excitation power we can use. The widths in frequency are defined while computing the correlations by grouping consecutive pixels in windows of different sizes with a minimum step size of 10.6  $\mu$ eV. 2PS are obtained by spanning the windows to compute all possible correlations, including partial and full-overlapping of the windows. This shows the considerable improvement of a streak-camera over standard setups with APDs. All the computations are done with the raw data only: there is no normalisation and the correlations go to 1 at long time self-consistently.

*Theory:* The fundamental dynamics of dissipation for a single harmonic oscillator  $a$  that mixes pure dephasing  $\gamma_\phi$  and radiative decay  $\gamma_a$  according to  $\partial_t \rho = [\frac{\gamma_a}{2} \mathcal{L}_a + \frac{\gamma_\phi}{2} \mathcal{L}_{a^\dagger a}] \rho$  with Lindblad terms  $\mathcal{L}_O \rho = 2O\rho O^\dagger - O^\dagger O \rho - \rho O^\dagger O$  for any operator  $O$ , can be solved exactly:

$$\rho_{n,m}(t) = \sum_{k=0}^{\infty} \rho_{k,m-n+k}(0) \sqrt{\binom{k}{n} \binom{m-n+k}{m}} (e^{\gamma_a t} - 1)^{k-n} e^{-[\gamma_a(2k+m-n) + \gamma_\phi(n-m)^2]t/2}, \quad (4)$$

with  $\rho_{n,m} = \langle n | \rho | m \rangle$  one element of the density matrix  $\rho$ . The time-integrated 2PS computed from Eq. (S1) can also be derived in closed-form (see the derivation of Eqs. (S36–S38) in the Supplementary Material):

$$\begin{aligned} \mathcal{F}_\Gamma^{(2)}(\omega_1, \omega_2) = \Re \Big\{ & \frac{(\gamma^2 + 4\omega_1^2)(\gamma^2 + 4\omega_2^2)}{2\gamma^2(\gamma + 2i\omega_2)} \left[ \frac{\gamma + 2\gamma_a}{(\gamma + 2\gamma_a)^2 + 4\omega_1^2} + \frac{\gamma_a}{\gamma + 2\gamma_a + 2i\omega_2} \right. \\ & \times \left( \frac{\gamma + 2\gamma_a - i(\omega_1 - \omega_2)}{(\gamma + 2\gamma_a - 2i\omega_1)(\Gamma + \gamma_a - i(\omega_1 - \omega_2))} + \frac{\gamma + 2\gamma_a + i(\omega_1 + \omega_2)}{(\gamma + 2\gamma_a + 2i\omega_1)(2\gamma - \Gamma - \gamma_a + i(\omega_1 + \omega_2))} \right) \Big] \Big\} \\ & + [1 \leftrightarrow 2], \quad (5) \end{aligned}$$

where  $\gamma = \Gamma + \gamma_a + \gamma_\phi$ . These results provide the complete dynamics of spontaneous emission of an arbitrary initial quantum state.

Our experiment realises—with an out-of-equilibrium polariton condensate maintained in a steady state through the interplay of pump and decay—a related though slightly more complex dynamics described at its most elementary

level by:

$$\frac{\partial \rho}{\partial t} = \left[ \frac{\gamma_a}{2} \mathcal{L}_a + \frac{\gamma_b}{2} \mathcal{L}_b + \frac{P_b}{2} \mathcal{L}_{b^\dagger} + \frac{P_{ba}}{2} \mathcal{L}_{a^\dagger b} \right] (\rho), \quad (6)$$

for the polariton condensate  $a$  and reservoir  $b$  lifetimes, reservoir pumping  $b^\dagger$  and particles transfer  $a^\dagger b$  from the reservoir to the condensate. Parameters are  $\gamma_a = \gamma_b$  throughout and  $P_{ba} = 10\gamma_a$ . The filter linewidth is  $\Gamma = \gamma_a/2$  throughout except in Fig. 3 where it spans  $\Gamma \in \{0.5, 0.75, 1, 5\}\gamma_a$ . The reservoir pumping  $P_b = \gamma_b$  throughout except Fig. 2 where it is also  $2\gamma_b$ . The 2PS is, in this case, obtained numerically, with full details of the procedure given in the Supplementary Material.

- 
- [1] Hanbury Brown, R. & Twiss, R. Q. A test of a new type of stellar interferometer on Sirius. *Nature* **178**, 1046 (1956).
  - [2] Glauber, R. J. Nobel lecture: One hundred years of light quanta. *Rev. Mod. Phys.* **78**, 1267 (2006).
  - [3] Weiner, R. M. *Introduction to Bose-Einstein Correlations and Subatomic Interferometry* (John Wiley & Sons Inc, 2000).
  - [4] Stevenson, R. M. *et al.* A semiconductor source of triggered entangled photon pairs. *Nature* **439**, 179 (2006).
  - [5] Jelts, T. *et al.* Comparison of the Hanbury Brown–Twiss effect for bosons and fermions. *Nature* **445**, 402 (2007).
  - [6] Ekert, A. K. Quantum cryptography based on bell’s theorem. *Phys. Rev. Lett.* **67**, 661 (1991).
  - [7] Cohen-Tannoudji, C. & Reynaud, S. Atoms in strong light-fields: Photon antibunching in single atom fluorescence. *Phil. Trans. R. Soc. Lond. A* **293**, 223 (1979).
  - [8] Nienhuis, G. Spectral correlations in resonance fluorescence. *Phys. Rev. A* **47**, 510 (1993).
  - [9] Dalibard, J. & Reynaud, S. Correlation signals in resonance fluorescence : interpretation via photon scattering amplitudes. *J. Phys. France* **44**, 1337 (1983).
  - [10] Knöll, L. & Weber, G. Theory of  $n$ -fold time-resolved correlation spectroscopy and its application to resonance fluorescence radiation. *J. Phys. B.: At. Mol. Phys.* **19**, 2817 (1986).
  - [11] Akopian, N. *et al.* Entangled photon pairs from semiconductor quantum dots. *Phys. Rev. Lett.* **96**, 130501 (2006).
  - [12] Hennessy, K. *et al.* Quantum nature of a strongly coupled single quantum dot–cavity system. *Nature* **445**, 896 (2007).
  - [13] Kaniber, M. *et al.* Investigation of the nonresonant dot-cavity coupling in two-dimensional photonic crystal nanocavities. *Phys. Rev. B* **77**, 161303(R) (2008).
  - [14] Sallen, G. *et al.* Subnanosecond spectral diffusion measurement using photon correlation. *Nat. Photon.* **4**, 696 (2010).
  - [15] Ulhaq, A. *et al.* Cascaded single-photon emission from the Mollow triplet sidebands of a quantum dot. *Nat. Photon.* **6**, 238 (2012).
  - [16] Deutsch, Z., Schwartz, O., Tenne, R., Popovitz-Biro, R. & Oron, D. Two-color antibunching from band-gap engineered colloidal semiconductor nanocrystals. *Nano Lett.* **12**, 2948 (2012).
  - [17] Gonzalez-Tudela, A., Laussy, F. P., Tejedor, C., Hartmann, M. J. & del Valle, E. Two-photon spectra of quantum emitters. *New J. Phys.* **15**, 033036 (2013).
  - [18] del Valle, E., Gonzalez-Tudela, A., Laussy, F. P., Tejedor, C. & Hartmann, M. J. Theory of frequency-filtered and time-resolved  $n$ -photon correlations. *Phys. Rev. Lett.* **109**, 183601 (2012).
  - [19] Kavokin, A., Baumberg, J. J., Malpuech, G. & Laussy, F. P. *Microcavities* (Oxford University Press, 2011), 2 edn.
  - [20] Wiersig, J. *et al.* Direct observation of correlations between individual photon emission events of a microcavity laser. *Nature* **460**, 245 (2009).
  - [21] Laussy, F. P., Malpuech, G., Kavokin, A. & Bigenwald, P. Spontaneous coherence buildup in a polariton laser. *Phys. Rev. Lett.* **93**, 016402 (2004).
  - [22] Holland, M., Burnett, K., Gardiner, C., Cirac, J. I. & Zoller, P. Theory of an atom laser. *Phys. Rev. A* **54**, R1757 (1996).
  - [23] Bartlett, S. D., Rudolph, T. & Spekkens, R. W. Reference frames, superselection rules, and quantum information. *Rev. Mod. Phys.* **79**, 555 (2007).
  - [24] Lvovsky, A. I. & Raymer, M. G. Continuous-variable optical quantum-state tomography. *Rev. Mod. Phys.* **81**, 299 (2009).
  - [25] Bocquillon, E. *et al.* Electron quantum optics in ballistic chiral conductors. *Annalen der Physik* **526**, 1 (2014).
  - [26] Sanchez Muñoz, C., del Valle, E., Tejedor, C. & Laussy, F. Violation of classical inequalities by photon frequency filtering. *Phys. Rev. A* **90**, 052111 (2014).
  - [27] Love, A. P. D. *et al.* Intrinsic decoherence mechanisms in the microcavity polariton condensate. *Phys. Rev. Lett.* **101**, 067404 (2008).
  - [28] Kasprzak, J. *et al.* Second-order time correlations within a polariton Bose–Einstein condensate in a CdTe microcavity. *Phys. Rev. Lett.* **100**, 067402 (2008).
  - [29] Aßmann, M. *et al.* From polariton condensates to highly photonic quantum degenerate states of bosonic matter. *Proc. Natl. Acad. Sci.* **108**, 1804 (2011).
  - [30] Centeno Neelen, R., Boersma, D. M., van Exter, M. P., Nienhuis, G. & Woerdman, J. P. Spectral filtering within the Schawlow–Townes linewidth as a diagnostic tool for studying laser phase noise. *Opt. Commun.* **100**, 289 (1993).
  - [31] Sanchez Muñoz, C. *et al.* Emitters of  $N$ -photon bundles. *Nat. Photon.* **8**, 550 (2014).
  - [32] del Valle, E. Distilling one, two and entangled pairs of photons from a quantum dot with cavity QED effects and spectral filtering. *New J. Phys.* **15**, 025019 (2013).

- [33] Koch, M. *et al.* Three-photon correlations in a strongly driven atom-cavity system. *Phys. Rev. Lett.* **107**, 023601 (2011).
- [34] Rundquist, A. *et al.* Nonclassical higher-order photon correlations with a quantum dot strongly coupled to a photonic-crystal nanocavity. *Phys. Rev. A* **90**, 023846 (2014).
- [35] Lang, C. *et al.* Observation of resonant photon blockade at microwave frequencies using correlation function measurements. *Phys. Rev. Lett.* **106**, 243601 (2011).
- [36] Eberly, J. & Wódkiewicz, K. The time-dependent physical spectrum of light. *J. Opt. Soc. Am.* **67**, 1252 (1977).
- [37] Laussy, F. *Exciton-polaritons in microcavities*, vol. 172, chap. 1. Quantum Dynamics of Polariton Condensates, 1–42 (Springer Berlin Heidelberg, 2012).
- [38] del Valle, E. *et al.* Dynamics of the formation and decay of coherence in a polariton condensate. *Phys. Rev. Lett.* **103**, 096404 (2009).
- [39] While there are various types of dephasing, we will consider with little loss of generality the simplest and most common type, known as “pure dephasing”.

### Acknowledgements

We thank Guillermo Guirales Arredondo for assistance with Fig. 1 and Juan Camilo López Carreño for discussions. This work has been funded by the ERC Grant POLAFLOW and the IEF project SQUIRREL (623708). AGT acknowledges support from the Alexander Von Humboldt Foundation, C.S.M. from a FPI grant and F.P.L. a RyC contract.

### Author contributions

DS, DB and MdG designed the experiment. KWW and LP grew the sample. BS and DB performed the experiment. GG provided experimental support and equipment. EdV, AGT, CSM and FPL proposed the theoretical model. AGT integrated the master equation. CSM optimized the computer code with which BS post-processed and analyzed the data. FPL wrote the main text. DS supervised the experiment and FPL and EdV the theory. All the authors contributed to writing the manuscript and discussed the results and their implications.

### Author Information

Authors declare no competing interest.

Correspondence and requests for materials should be addressed to fabrice.laussy@gmail.com

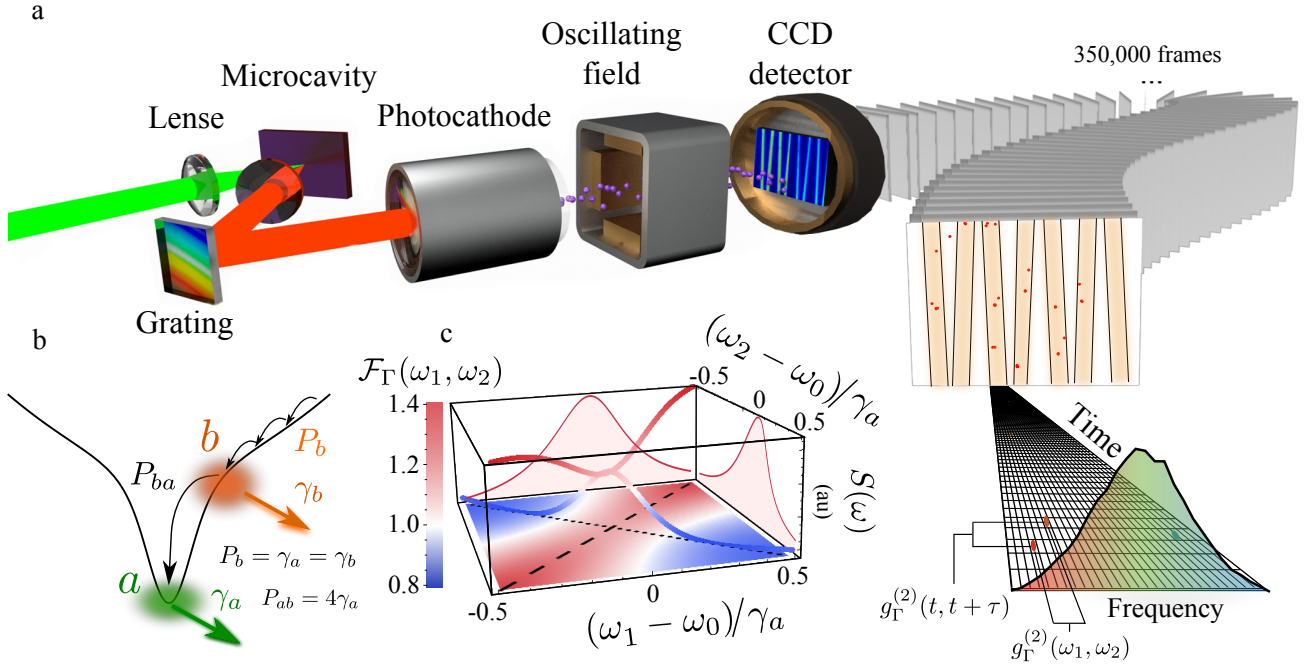


FIG. 1: **Principle and Setup of time- and frequency-resolved photon correlations.** (a) Sketch of the experiment: the reflected light from a microcavity is dispersed onto a streak-camera detecting at the single-photon level and stored in individual frames which post-processing allows to build photon-correlation landscapes (b) Sketch of the theory: a laser excites non-resonantly the lower polariton dispersion, creating a reservoir of hot excitons  $b$  that condense into the ground state  $a$  at the minimum of the branch. (c) Bosonic form factor  $\mathcal{F}(\omega_1, \omega_2)$ , i.e., time-integrated 2PS for the spontaneous emission of a coherent state with  $g^{(2)} = 1$ , providing the backbone for the experiment. The diagonal and antidiagonal exhibit bunching and antibunching, respectively.

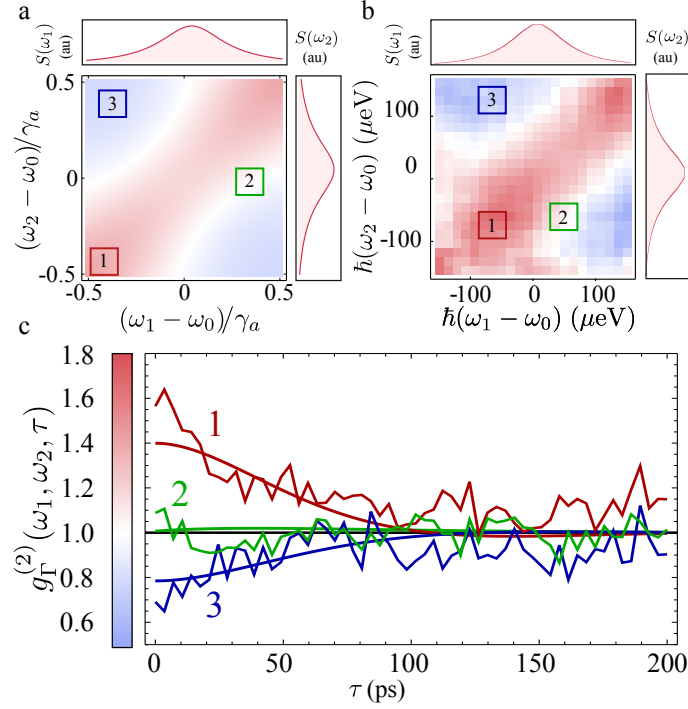


FIG. 2: **Two-photon correlations spectra.** (a) Theoretical calculation of  $g_{\Gamma}^{(2)}(\omega_1, \omega_2; 0)$  for the spontaneous emission from a steady-state polariton condensate, qualitatively similar to the bosonic form factor. (b) Experimental observation of  $g_{\Gamma}^{(2)}(\omega_1, \omega_2; 0)$  in the same regime, displaying a remarkable agreement. (c) Time-resolved correlation for the three regions marked in the colour map: (i) on the diagonal ( $\omega_1 = \omega_2$ ) exhibiting bunching, (ii) in the region of transition with no correlation, (iii) correlating opposing elbows, exhibiting antibunching.

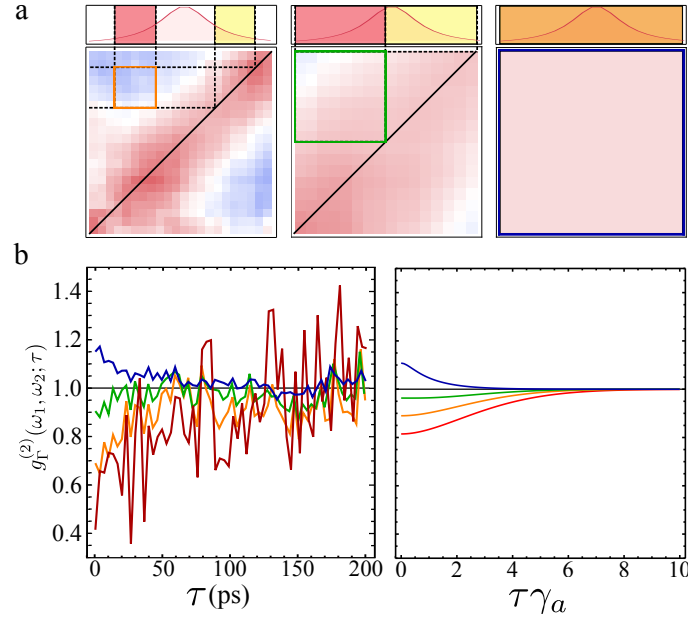


FIG. 3: **Effect of detectors linewidths.** (a) Two-photon correlation landscapes  $g_{\Gamma}^{(2)}(\omega_1, \omega_2; 0)$  as a function of the filter width, from a fraction of the peak, 74.1 μeV (left), roughly half-peak width, 158.8 μeV (center), to full-peak filtering, corresponding to standard auto-correlations. The position of the two filters is shown explicitly on the spectral line as the red and yellow windows (orange when overlapping). (b) Time-resolved correlation for the selected areas. The smallest frequency window available, 10.6 μeV, is shown in red: antibunching is even more pronounced although the signal becomes extremely noisy.



# Measuring photon correlations simultaneously in time and frequency

## Supplementary Material.

### A. Frequency correlations of quantum states

The formal theory of time and frequency resolved correlations is well-established since the 80s<sup>7-10</sup>. The two-photon frequency correlations is expressed as (Eq. (2) of the text):

$$g_{\Gamma}^{(2)}(\omega_1, T_1; \omega_2, T_2) = \frac{\langle : \mathcal{T} [\prod_{i=1}^2 A_{\omega_i, \Gamma}^{\dagger}(T_i) A_{\omega_i, \Gamma}(T_i)] : \rangle}{\prod_{i=1}^2 \langle A_{\omega_i, \Gamma}^{\dagger}(T_i) A_{\omega_i, \Gamma}(T_i) \rangle} \quad (\text{S1})$$

where:

$$A_{\omega_i, \Gamma}(T_i) = \int_{-\infty}^{T_i} e^{i\omega_i t} e^{-\Gamma(T_i-t)/2} a(t) dt \quad (\text{S2})$$

is the field of frequency component  $\omega_i$  and width  $\Gamma$ , at time  $T_i$ , and  $\mathcal{T}$ , (resp.  $:$ ) refer to time (resp. normal) ordering. This must be contrasted with the conventional second-order correlation function:

$$g_0^{(2)} = \frac{\sum_{n=0}^{\infty} n(n-1) \langle n | \rho | n \rangle}{(\sum_{n=0}^{\infty} n \langle n | \rho | n \rangle)^2}, \quad (\text{S3})$$

that only requires the density matrix  $\rho$  to be computed. On the other hand, for  $g^{(2)}(\omega_1, T_1; \omega_2, T_2)$ , one needs the time dynamics even to compute zero-delay coincidences with  $T_1 = T_2$  since one has to integrate over time  $t$ , as seen in Eq. (S2). When including the frequency information, one must therefore specify which dynamics is bringing the photons from the state towards the detectors that will correlate them. The fact that such basic physical processes are required to compute the 2PS shows that it is more fundamental in character than the conventional  $g^{(2)}$ . This is similar to early descriptions by Eberly and Wódkiewicz<sup>36</sup> of photoluminescence spectra of light beyond the Wiener-Khintchin theorem, that presupposes no emission. Here too, the necessity to take into account emission and detection of the photons to define a physical spectrum of light was pointed out.

The most basic process to bring a photon from the quantum state toward a detector is spontaneous emission, followed by free propagation toward the detector that performs the frequency-filtering and correlation. This provides us with the simplest dynamics to which one can subject the time evolution of the quantum state of an harmonic oscillator, as ruled by the master equation for its density matrix:

$$\frac{\partial \rho}{\partial t} = \left[ \frac{\gamma_a}{2} \mathcal{L}_a + \frac{\gamma_{\phi}}{2} \mathcal{L}_{a^{\dagger}a} \right] (\rho). \quad (\text{S4})$$

We have also included pure dephasing, for reasons explained in the main text. The equation can be integrated in closed form for  $\rho_{n,m} = \langle n | \rho | m \rangle$  which takes the form:

$$\dot{\rho}_{n,m} = -\frac{1}{2} [\gamma_a(n+m) + \gamma_{\phi}(n-m)^2] \rho_{n,m} + \gamma_a \sqrt{(m+1)(n+1)} \rho_{n+1,m+1}, \quad (\text{S5})$$

and that can be solved by recurrence, to yield Eq. (4) of the main text. From  $\rho(t)$ , one can compute all single-time observables, such as the population:

$$n(t) = \langle a^{\dagger}a \rangle(t) = n(0) \exp(-\gamma_a t), \quad (\text{S6})$$

i.e., simple exponential decay, as expected on physical grounds and despite the complicated form of the general solution. The two-photon correlation:

$$g^{(2)}(t) = \frac{\langle a^{\dagger}a^{\dagger}aa \rangle(t)}{\langle a^{\dagger}a \rangle(t)^2}. \quad (\text{S7})$$

provides an even simpler and stronger result:

$$g^{(2)}(t) = g^{(2)}(0). \quad (\text{S8})$$

The photon-statistics is constant with time. One can also compute the two-times correlation function (Eq. (1) of the main text) through the quantum regression theorem (demonstration not given), and find a similarly constrained result:

$$g^{(2)}(t, \tau) = g^{(2)}(0, 0). \quad (\text{S9})$$

This implies, for instance,  $\lim_{\tau \rightarrow \infty} g^{(2)}(t, \tau) \neq 1$  for most of the cases, i.e., photons are always correlated. This is reasonable since any two photons emitted by the system come from the same and only initial state which is let to evolve at precisely  $t = 0$ .

Since we are dealing with many closely related variations of  $g^{(2)}$ , we will use the following definition for what is the central quantity of this work, the zero-delay (coincidence) second order correlation function:

$$g_0^{(2)} \equiv g^{(2)}(t = 0, \tau = 0). \quad (\text{S10})$$

This quantity is usually found in the literature written as  $g^{(2)}(0)$ .

We now compute the two-photon correlations from an initial state when including the frequency degree of freedom. To keep the discussion as fundamental and simple as possible, we consider here the time-integrated case that disposes of time altogether:

$$g_\Gamma^{(2)}(\omega_1, \omega_2) = \frac{\int_0^\infty \langle n_1(t_1) n_2(t_2) \rangle dt_1 dt_2}{\int_0^\infty \langle n_1(t_1) \rangle dt_1 \int_0^\infty \langle n_2(t_2) \rangle dt_2} \quad (\text{S11})$$

where  $n_i = A_{\omega_i, \Gamma}^\dagger A_{\omega_i, \Gamma}$  for  $i = 1, 2$  are sensors detecting in the corresponding spectral windows<sup>18</sup>. This is equivalent to letting the detectors gather statistical information from photons detected at any time, hence reconstructing the frequency of the photons with full precision. This quantity is the closest one to what an actual experiment would perform, although other configurations are possible (they would bring us to an essentially identical discussion and conclusions). Applying Eq. (S11) to the case of free propagation only ( $\gamma_a = 0$  and  $\gamma_\phi = 0$ ) is pathological because the energy is then exactly determined and frequency correlations becomes trivial or ill-defined in terms of  $\delta$  functions. The simplest physically sound dynamics is that of a free field that, at least, decays ( $\gamma_a \neq 0$  and  $\gamma_\phi = 0$ ). One can then compute a physical frequency-correlation spectrum, and interpret the photons annihilated by the decay as those detected by the apparatus to register the information required to compute the correlations. In this case, corresponding to spontaneous emission of the state, the result is the same for frequencies as Eq. (S9):

$$g_\Gamma^{(2)}(\omega_1, \omega_2) = g_0^{(2)}, \quad (\text{S12})$$

as will be shown in next Section. The physical reason for this behaviour is explained in the main text. Including dephasing on top of the radiative decay ( $\gamma_a \neq 0$  and  $\gamma_\phi \neq 0$ ) brings us to the result:

$$g_\Gamma^{(2)}(\omega_1, \omega_2) = g_0^{(2)} \mathcal{F}_\Gamma(\omega_1, \omega_2), \quad (\text{S13})$$

with  $\mathcal{F}_\Gamma(\omega_1, \omega_2)$  a *boson form factor*, which is independent of the quantum state  $\rho$  in which the system is prepared, and depends only on the dynamics of emission and detection. The previous result, Eq. (S12), follows from  $\mathcal{F}_\Gamma(\omega_1, \omega_2)$  being unity when  $\gamma_\phi = 0$ .

In general, when the physics goes beyond that of the mere emission from a quantum state  $\rho$ , and involves virtual processes, dressing of the states, collective emission, stimulated emission and other types of likewise quantum correlations, the standard Glauber's correlation  $g_0^{(2)}$  does not simply factorize from  $g_\Gamma^{(2)}(\omega_1, \omega_2)$ . In such cases, the 2PS offers a complex landscape of correlations with strong and characteristic features<sup>17</sup>, that can be taken advantage of for distillation<sup>32</sup>, strongly-correlated emission<sup>31</sup> and quantum information processing<sup>26</sup>. This is however experimentally outside the scope of this paper which makes the first step in these exciting directions by confirming Eq. (S13).

## B. Calculation of the Boson form factor.

We now detail the calculation of  $\mathcal{F}_\Gamma(\omega_1, \omega_2)$ . Let us assume a quantum system described by a set of operators  $a$ ,  $\sigma$ , etc., acting in a Hilbert space  $\mathcal{H}$ . In second quantization, these operators define annihilation operators in the Heisenberg picture. All single-time quantities can be obtained from correlators of the type  $\langle a^{\dagger\mu} a^\nu \sigma^{\dagger\eta} \sigma^\theta \dots \rangle$  with  $\mu$ ,  $\nu$ ,  $\eta$ ,  $\theta$ , etc., integers. Let us call  $\mathcal{O}$  the set of operators the averages of which correspond to the correlators required to describe the system, i.e.,  $\mathcal{O}$  includes all the sought observables as well as operators which couple to them through the equations of motion. In the following, we assume, without loss of generality, that  $a$  is the mode of interest, the correlations of which are to be computed in time and frequency during its decaying time dynamics.

We define the time-dependent vector  $\mathbf{v}$  as:

$$\mathbf{v} = \begin{pmatrix} 1 \\ \langle a \rangle(t) \\ \langle a^\dagger \rangle(t) \\ \langle a^\dagger a \rangle(t) \\ \vdots \end{pmatrix}, \quad (\text{S14})$$

composed of the mean values of all relevant operators in  $\mathcal{O}$  taken in some order, which will be kept for the remainder of the text as starting with the sequence  $\mathcal{O} = \{1, a, a^\dagger, a^\dagger a, \dots\}$ . From the master equation, one can define for  $\mathcal{O}$  a matrix  $M$  which rules the dynamical evolution of  $\mathbf{v}$ :  $\partial_t \mathbf{v} = M \mathbf{v}$ , with solution  $\mathbf{v} = e^{Mt} \mathbf{v}_0$  and integrated value  $\bar{\mathbf{v}} = \int_0^\infty e^{-\lambda t} \mathbf{v} dt = \int_0^\infty e^{-\lambda t} e^{Mt} \mathbf{v}_0 dt = \frac{-1}{M - \lambda \mathbf{1}} \mathbf{v}_0$ . Note that  $M$  is typically singular, i.e.,  $|M| = 0$ , therefore we include an exponential decay  $e^{-\lambda t}$  that forces the dynamics to die away so that we can enforce  $\lim_{t \rightarrow \infty} e^{-\lambda t} \mathbf{v} = 0$ . At the end of the calculations we take the limit  $\lambda \rightarrow 0$ .

We now consider two sensors  $\varsigma_i$ ,  $i = 1, 2$  with linewidths  $\Gamma_i$  coupled to the system with strength  $\varepsilon_i$  such that the dynamics of the system is probed but is otherwise left unperturbed. We then introduce a sensing vector  $\mathbf{w}$  of steady state correlators, by multiplying  $\varsigma_1^{\dagger \mu_1} \varsigma_1^{\nu_1} \varsigma_2^{\dagger \mu_2} \varsigma_2^{\nu_2}$  with the operators in  $\mathcal{O}$ :

$$\mathbf{w}[\mu_1 \nu_1, \mu_2 \nu_2] = \begin{pmatrix} \langle \varsigma_1^{\dagger \mu_1} \varsigma_1^{\nu_1} \varsigma_2^{\dagger \mu_2} \varsigma_2^{\nu_2} \rangle(t) \\ \langle \varsigma_1^{\dagger \mu_1} \varsigma_1^{\nu_1} \varsigma_2^{\dagger \mu_2} \varsigma_2^{\nu_2} a \rangle(t) \\ \langle \varsigma_1^{\dagger \mu_1} \varsigma_1^{\nu_1} \varsigma_2^{\dagger \mu_2} \varsigma_2^{\nu_2} a^\dagger \rangle(t) \\ \langle \varsigma_1^{\dagger \mu_1} \varsigma_1^{\nu_1} \varsigma_2^{\dagger \mu_2} \varsigma_2^{\nu_2} a^\dagger a \rangle(t) \\ \vdots \end{pmatrix}, \quad (\text{S15})$$

where the indices  $\mu_i$  and  $\nu_i$  take the values 0 or 1. The integrated quantity is denoted  $\bar{\mathbf{w}}[\mu_1 \nu_1, \mu_2 \nu_2] = \int_0^\infty e^{-\lambda t} \mathbf{w}[\mu_1 \nu_1, \mu_2 \nu_2] dt$ . Furthermore, we also introduce the two-time correlator vector as:

$$\mathbf{w}'[\mu_1 \nu_1, \mu_2 \nu_2] = \begin{pmatrix} \langle (\varsigma_1^{\dagger \mu_1} \varsigma_1^{\nu_1})(t) (\varsigma_2^{\dagger \mu_2} \varsigma_2^{\nu_2})(t + \tau) \rangle \\ \langle (\varsigma_1^{\dagger \mu_1} \varsigma_1^{\nu_1})(t) (\varsigma_2^{\dagger \mu_2} \varsigma_2^{\nu_2} a)(t + \tau) \rangle \\ \langle (\varsigma_1^{\dagger \mu_1} \varsigma_1^{\nu_1})(t) (\varsigma_2^{\dagger \mu_2} \varsigma_2^{\nu_2} a^\dagger)(t + \tau) \rangle \\ \langle (\varsigma_1^{\dagger \mu_1} \varsigma_1^{\nu_1})(t) (\varsigma_2^{\dagger \mu_2} \varsigma_2^{\nu_2} a^\dagger a)(t + \tau) \rangle \\ \vdots \end{pmatrix}, \quad (\text{S16})$$

with a two-time integral as  $\bar{\bar{\mathbf{w}}}[\mu_1 \nu_1, \mu_2 \nu_2] = \iint_0^\infty e^{-\lambda t} e^{-\lambda \tau} \mathbf{w}'[\mu_1 \nu_1, \mu_2 \nu_2] dt d\tau$ . Finally, we define two matrices,  $T_\pm$ , which, when acting on  $\mathbf{v}$  or  $\mathbf{w}$ , introduce an extra  $a^\dagger$  for  $T_+$  and an  $a$  for  $T_-$ , keeping normal ordering. These matrices always exist, in infinite or in truncated Hilbert spaces (where, if truncation is to order  $n$ ,  $a^n$  is an operator in  $\mathcal{O}$  but  $a^{n+1} = 0$ ).

In the regime under consideration, the population  $\langle \varsigma_i^\dagger \varsigma_i \rangle \ll 1$  and the equations of motion are valid to leading order in  $\varepsilon_{1,2}$ :

$$\begin{aligned} \partial_t \mathbf{w}[\mu_1 \nu_1, \mu_2 \nu_2] = & \{M + [(\mu_1 - \nu_1)i\omega_1 - (\mu_1 + \nu_1)\frac{\Gamma_1}{2} + (\mu_2 - \nu_2)i\omega_2 - (\mu_2 + \nu_2)\frac{\Gamma_2}{2}]\mathbf{1}\} \mathbf{w}[\mu_1 \nu_1, \mu_2 \nu_2] \\ & + \mu_1(i\varepsilon_1 T_+) \mathbf{w}[0 \nu_1, \mu_2 \nu_2] + \nu_1(-i\varepsilon_1 T_-) \mathbf{w}[\mu_1 0, \mu_2 \nu_2] + \mu_2(i\varepsilon_2 T_+) \mathbf{w}[\mu_1 \nu_1, 0 \nu_2] + \nu_2(-i\varepsilon_2 T_-) \mathbf{w}[\mu_1 \nu_1, \mu_2 0]. \end{aligned} \quad (\text{S17})$$

Since the sensors are empty at  $t = 0$  and at  $t = \infty$  ( $\bar{w}(0(\infty)) \equiv 0$ ), we easily obtain the solution for  $\bar{\mathbf{w}}$  by formal integration of these equations, noting that  $\int_0^\infty e^{-\lambda t} \partial_t \mathbf{w} dt = \lambda \bar{\mathbf{w}}$ :

$$\begin{aligned} \bar{\mathbf{w}}[\mu_1 \nu_1, \mu_2 \nu_2] = & \frac{-1}{M + [(\mu_1 - \nu_1)i\omega_1 - (\mu_1 + \nu_1)\frac{\Gamma_1}{2} + (\mu_2 - \nu_2)i\omega_2 - (\mu_2 + \nu_2)\frac{\Gamma_2}{2} - \lambda]\mathbf{1}} \\ & \times \left\{ \mu_1(i\varepsilon_1 T_+) \bar{\mathbf{w}}[0 \nu_1, \mu_2 \nu_2] + \nu_1(-i\varepsilon_1 T_-) \bar{\mathbf{w}}[\mu_1 0, \mu_2 \nu_2] + \mu_2(i\varepsilon_2 T_+) \bar{\mathbf{w}}[\mu_1 \nu_1, 0 \nu_2] + \nu_2(-i\varepsilon_2 T_-) \bar{\mathbf{w}}[\mu_1 \nu_1, \mu_2 0] \right\}. \end{aligned} \quad (\text{S18})$$

This produces exactly the same type or recursive relation between the integrated correlators that one has in the case of a steady state (under continuous pumping)<sup>18</sup>. The only difference appears when reaching the last vector in the recursive chain, that now is given by  $\bar{\mathbf{w}}[00, 00] = \bar{\mathbf{v}}$  instead of the steady state value.

For the two-time correlator, we have:

$$\begin{aligned} \partial_\tau \mathbf{w}'[\mu_1 \nu_1, \mu_2 \nu_2] = & \{M + [(\mu_2 - \nu_2)i\omega_2 - (\mu_2 + \nu_2)\frac{\Gamma_2}{2}]\mathbf{1}\} \mathbf{w}'[\mu_1 \nu_1, \mu_2 \nu_2] \\ & + \mu_2(i\varepsilon_2 T_+) \mathbf{w}'[\mu_1 \nu_1, 0 \nu_2] + \nu_2(-i\varepsilon_2 T_-) \mathbf{w}'[\mu_1 \nu_1, \mu_2 0]. \end{aligned} \quad (\text{S19})$$

The formal double integration of these equations, noting that  $\iint_0^\infty e^{-\lambda t} e^{-\lambda \tau} \partial_\tau \mathbf{w}' dt d\tau = -\bar{\bar{\mathbf{w}}} + \lambda \bar{\bar{\mathbf{w}}}'$ , leads to:

$$\begin{aligned} \bar{\bar{\mathbf{w}}}'[\mu_1 \nu_1, \mu_2 \nu_2] = & \frac{-1}{M + [(\mu_2 - \nu_2)i\omega_2 - (\mu_2 + \nu_2)\frac{\Gamma_2}{2} - \lambda]\mathbf{1}} \\ & \times \left\{ \mu_2(i\varepsilon_2 T_+) \bar{\bar{\mathbf{w}}}'[\mu_1 \nu_1, 0 \nu_2] + \nu_2(-i\varepsilon_2 T_-) \bar{\bar{\mathbf{w}}}'[\mu_1 \nu_1, \mu_2 0] + \bar{\mathbf{w}}[\mu_1 \nu_1, \mu_2 \nu_2] \right\}. \end{aligned} \quad (\text{S20})$$

The final correlator in the recursive chain is given by  $\mathbf{w}'[\mu_1\nu_1, 00] = e^{M\tau}\mathbf{w}[\mu_1\nu_1, 00]$  and the integral, therefore, by:

$$\overline{\overline{\mathbf{w}}}'[\mu_1\nu_1, 00] = \frac{-1}{M - \lambda\mathbf{1}}\overline{\mathbf{w}}[\mu_1\nu_1, 00]. \quad (\text{S21})$$

At this stage we are ready to obtain the single-photon and two-photon spectra. The Eberly or time-dependent spectrum of emission of  $a$  is given by the average population of any one of the two sensors, say,  $\langle n_1 \rangle = \langle \varsigma_1^\dagger \varsigma_1 \rangle(t)$ . Its equation of motion reads  $\partial_t \langle n_1 \rangle = -\Gamma_1 \langle n_1 \rangle + 2\Re(i\varepsilon_1 \langle \varsigma_1 a^\dagger \rangle(t))$ , and with the above notations, the total integrated spectrum is therefore given by:

$$\overline{\langle n_1 \rangle} = \lim_{\lambda \rightarrow 0} \frac{2}{\Gamma_1} \Re \left[ i\varepsilon_1 T_+ \overline{\mathbf{w}}[01, 00] \right]_1. \quad (\text{S22})$$

The subindex in  $[\cdot]_1$  means taking the first element of the resulting vector. Using the solution Eq. (S18), the correlator of interest for the spectrum reads:

$$\overline{\mathbf{w}}[01, 0, 0] = \frac{-1}{M + [-i\omega_1 - \frac{\Gamma_1}{2} - \lambda]\mathbf{1}} (-i\varepsilon_1 T_-) \overline{\mathbf{v}}. \quad (\text{S23})$$

The two-photon spectrum follows similarly. The integral of the intensity correlations between two sensors,  $\langle n_1(t_1)n_2(t_2) \rangle = \langle (\varsigma_1^\dagger \varsigma_1)(t_1)(\varsigma_2^\dagger \varsigma_2)(t_2) \rangle$ , is given by  $\int \int_0^\infty \langle n_1(t_1)n_2(t_2) \rangle dt_1 dt_2 = \lim_{\lambda \rightarrow 0} \overline{\langle n_1 n_2 \rangle} + [1 \leftrightarrow 2]$  where  $\overline{\langle n_1 n_2 \rangle} = \int \int_0^\infty e^{-\lambda t} e^{-\lambda \tau} \langle n_1(t)n_2(t+\tau) \rangle dt d\tau$  and  $[1 \leftrightarrow 2]$  means to exchange sensor parameters in the previous expression. The correlator of interest,  $\langle n_1(t)n_2(t+\tau) \rangle$ , with equation of motion:

$$\partial_\tau \langle n_1(t)n_2(t+\tau) \rangle = -\Gamma_2 \langle n_1(t)n_2(t+\tau) \rangle + 2\Re \left[ i\varepsilon_2 \langle n_1(t)(\varsigma_2 a^\dagger)(t+\tau) \rangle \right], \quad (\text{S24})$$

relies on the vectors  $\mathbf{w}'[11, \mu_2\nu_2]$ . In particular,  $\langle n_1(t)(\varsigma_2 a^\dagger)(t+\tau) \rangle$  is the first element of the vector  $T_+ \mathbf{w}'[11, 01]$ . The integrated correlator reads:

$$\overline{\langle n_1 n_2 \rangle} = \frac{1}{\Gamma_2 + \lambda} \left\{ \overline{\langle n_1 n_2 \rangle} + 2\Re \left[ i\varepsilon_2 T_+ \overline{\mathbf{w}}'[11, 01] \right]_1 \right\} \quad (\text{S25})$$

The one-time integrated correlator is given by:

$$\overline{\langle n_1 n_2 \rangle} = \frac{1}{\Gamma_1 + \Gamma_2 + \lambda} 2\Re \left[ i\varepsilon_2 T_+ \overline{\mathbf{w}}[11, 01] \right]_1 + [1 \leftrightarrow 2], \quad (\text{S26})$$

while the solution for  $\overline{\mathbf{w}}'[11, 01]$  is:

$$\overline{\mathbf{w}}'[11, 01] = \frac{-1}{M + (-i\omega_2 - \frac{\Gamma_2}{2} - \lambda)\mathbf{1}} \left\{ -i\varepsilon_2 T_- \overline{\mathbf{w}}'[11, 00] + \overline{\mathbf{w}}[11, 01] \right\}. \quad (\text{S27})$$

Altogether, using Eq. (S21), we get the final expression for the integrated correlations:

$$\begin{aligned} \int \int_0^\infty \langle n_1(t_1)n_2(t_2) \rangle dt_1 dt_2 &= \lim_{\lambda \rightarrow 0} \frac{2}{\Gamma_2} \Re \left[ (i\varepsilon_2 T_+) \left\{ \left[ \frac{1}{\Gamma_1} \mathbf{1} + \frac{-1}{M + (-i\omega_2 - \frac{\Gamma_2}{2})\mathbf{1}} \right] \overline{\mathbf{w}}[11, 01] \right. \right. \\ &\quad \left. \left. + \frac{-1}{M + (-i\omega_2 - \frac{\Gamma_2}{2})\mathbf{1}} (-i\varepsilon_2 T_-) \frac{-1}{M - \lambda\mathbf{1}} \overline{\mathbf{w}}[11, 00] \right\} \right]_1 + [1 \leftrightarrow 2]. \end{aligned} \quad (\text{S28})$$

The required vectors are given by the solutions:

$$\overline{\mathbf{w}}[11, 01] = \frac{-1}{M + (-i\omega_2 - \Gamma_1 - \frac{\Gamma_2}{2} - \lambda)\mathbf{1}} \left\{ -i\varepsilon_2 T_- \overline{\mathbf{w}}[11, 00] - i\varepsilon_1 T_- \overline{\mathbf{w}}[10, 01] + i\varepsilon_1 T_+ \overline{\mathbf{w}}[01, 01] \right\}, \quad (\text{S29})$$

with:

$$\overline{\mathbf{w}}[11, 00] = \frac{-1}{M + (-\Gamma_1 - \lambda)\mathbf{1}} \left\{ i\varepsilon_1 T_+ \overline{\mathbf{w}}[01, 00] - i\varepsilon_1 T_- \overline{\mathbf{w}}[10, 00] \right\}, \quad (\text{S30a})$$

$$\overline{\mathbf{w}}[10, 01] = \frac{-1}{M + (i\omega_1 - i\omega_2 - \frac{\Gamma_1 + \Gamma_2}{2} - \lambda)\mathbf{1}} \left\{ -i\varepsilon_2 T_- \overline{\mathbf{w}}[10, 00] + i\varepsilon_1 T_+ \overline{\mathbf{w}}[00, 01] \right\}, \quad (\text{S30b})$$

$$\mathbf{w}[01, 01] = \frac{-1}{M + (-i\omega_1 - i\omega_2 - \frac{\Gamma_1 + \Gamma_2}{2} - \lambda)\mathbf{1}} \left\{ -i\varepsilon_1 T_- \mathbf{w}[00, 01] - i\varepsilon_2 T_- \mathbf{w}[01, 00] \right\}. \quad (\text{S30c})$$

Finally:

$$\bar{\mathbf{w}}[10, 00] = \frac{-1}{M + (i\omega_1 - \frac{\Gamma_1}{2} - \lambda)\mathbf{1}} i\varepsilon_1 T_+ \bar{\mathbf{v}}, \quad (\text{S31a})$$

$$\bar{\mathbf{w}}[00, 01] = \frac{-1}{M + (-i\omega_2 - \frac{\Gamma_2}{2} - \lambda)\mathbf{1}} (-i\varepsilon_2 T_-) \bar{\mathbf{v}}, \quad (\text{S31b})$$

$$\bar{\mathbf{w}}[01, 00] = \frac{-1}{M + (-i\omega_1 - \frac{\Gamma_1}{2} - \lambda)\mathbf{1}} (-i\varepsilon_1 T_-) \bar{\mathbf{v}}. \quad (\text{S31c})$$

With this, we get the final formulas to include in Eq. (S28):

$$\begin{aligned} \bar{\mathbf{w}}[11, 01] = & -i\varepsilon_1^2 \varepsilon_2 \frac{1}{M + (-i\omega_2 - \Gamma_1 - \frac{\Gamma_2}{2} - \lambda)\mathbf{1}} \\ & \times \left\{ T_- \frac{1}{M + (-\Gamma_1 - \lambda)\mathbf{1}} \left( T_+ \frac{1}{M + (-i\omega_1 - \frac{\Gamma_1}{2} - \lambda)\mathbf{1}} T_- + T_- \frac{1}{M + (i\omega_1 - \frac{\Gamma_1}{2} - \lambda)\mathbf{1}} T_+ \right) \right. \\ & + T_- \frac{1}{M + (i\omega_1 - i\omega_2 - \frac{\Gamma_1 + \Gamma_2}{2} - \lambda)\mathbf{1}} \left( T_- \frac{1}{M + (i\omega_1 - \frac{\Gamma_1}{2} - \lambda)\mathbf{1}} T_+ + T_+ \frac{1}{M + (-i\omega_2 - \frac{\Gamma_2}{2} - \lambda)\mathbf{1}} T_- \right) \\ & \left. + T_+ \frac{1}{M + (-i\omega_1 - i\omega_2 - \frac{\Gamma_1 + \Gamma_2}{2} - \lambda)\mathbf{1}} T_- \left( \frac{1}{M + (-i\omega_2 - \frac{\Gamma_2}{2} - \lambda)\mathbf{1}} + \frac{1}{M + (-i\omega_1 - \frac{\Gamma_1}{2} - \lambda)\mathbf{1}} \right) T_- \right\} \frac{1}{M - \lambda\mathbf{1}} \mathbf{v}_0, \end{aligned} \quad (\text{S32})$$

and

$$\bar{\mathbf{w}}[11, 00] = -\varepsilon_1^2 \frac{1}{M + (-\Gamma_1 - \lambda)\mathbf{1}} \left( T_+ \frac{1}{M + (-i\omega_1 - \frac{\Gamma_1}{2} - \lambda)\mathbf{1}} T_- + T_- \frac{1}{M + (i\omega_1 - \frac{\Gamma_1}{2} - \lambda)\mathbf{1}} T_+ \right) \frac{1}{M - \lambda\mathbf{1}} \mathbf{v}_0. \quad (\text{S33})$$

All the previous derivation has been kept at a general level, that could be applied to the spontaneous emission of any system. We now apply it to the case of interest for our previous discussion, namely, the case of an harmonic oscillator with decay and pure dephasing, cf. Eq. (S4). In this simple case, the vector  $\mathbf{v}$  needed to compute correlators up to second order, truncates naturally at  $\langle a^\dagger a^\dagger a a \rangle$  with only 9 elements. The corresponding matrix  $M$  is diagonal. The time integrated spectrum of emission reduces to simply:

$$\int_0^\infty \langle n_1(t_1) \rangle dt_1 = \varepsilon^2 \frac{2}{\Gamma\gamma_a} \frac{\gamma/2}{(\gamma/2)^2 + \omega_1^2} n_0, \quad (\text{S34})$$

with  $n_0$  the initial population of the harmonic mode and  $\gamma = \Gamma + \gamma_a + \gamma_\phi$  (we also took the coupling to sensors and their decay rates equal for simplicity) and taking the limit  $\lambda \rightarrow 0$ . The integrated correlations can be derived similarly, to provide the more complex expression:

$$\begin{aligned} \iint_0^\infty \langle n_1(t_1) n_2(t_2) \rangle dt_1 dt_2 = & n_0^2 g_0^{(2)} \varepsilon^4 \Re \left\{ \frac{8}{\Gamma^2 \gamma_a^2 (\gamma + 2i\omega_2)} \left[ \frac{\gamma + 2\gamma_a}{(\gamma + 2\gamma_a)^2 + 4\omega_1^2} + \frac{\gamma_a}{\gamma + 2\gamma_a + 2i\omega_2} \right. \right. \\ & \left. \left. \times \left( \frac{\gamma + 2\gamma_a - i(\omega_1 - \omega_2)}{(\gamma + 2\gamma_a - 2i\omega_1)(\Gamma + \gamma_a - i(\omega_1 - \omega_2))} + \frac{\gamma + 2\gamma_a + i(\omega_1 + \omega_2)}{(\gamma + 2\gamma_a + 2i\omega_1)(2\gamma - \Gamma - \gamma_a + i(\omega_1 + \omega_2))} \right) \right] \right\} + [1 \leftrightarrow 2], \end{aligned} \quad (\text{S35})$$

which, according to Eq. (S13), finally provides the analytical expression for the frequency-resolved two-photon spectrum of spontaneous emission of an arbitrary quantum state of the harmonic oscillator with pure dephasing:

$$g_\Gamma^{(2)}(\omega_1, \omega_2) = \frac{\iint_0^\infty \langle n_1(t_1) n_2(t_2) \rangle dt_1 dt_2}{\int_0^\infty \langle n_1(t_1) \rangle dt_1 \int_0^\infty \langle n_2(t_2) \rangle dt_2} = g_0^{(2)} \mathcal{F}_\Gamma(\omega_1, \omega_2). \quad (\text{S36})$$

The exact expression for  $\mathcal{F}_\Gamma(\omega_1, \omega_2)$  follows straightforwardly from Eqs. (S34) & (S35) and is written in a self-contained way as Eq. (5) of the main text in the Methods section. It is plotted in Fig. 2c of the main text. This form factor fullfils the following limits:  $\lim_{\Gamma \rightarrow \infty} \mathcal{F}_\Gamma(\omega_1, \omega_2) = 1$  (we recover the total integrated correlations when opening the window to include all the frequencies) and  $\lim_{\gamma_\phi \rightarrow 0} \mathcal{F}_\Gamma(\omega_1, \omega_2) = 1$  (without pure dephasing the 2PS lacks any structure in frequency). More notably  $\lim_{\Gamma \rightarrow 0} \lim_{\gamma_\phi \rightarrow \infty} \mathcal{F}_\Gamma(\omega_1, \omega_2) = 1 + \delta_{\omega_1, \omega_2}$ , which recovers indistinguishability bunching, the factor 2! for equal frequencies, and otherwise uncorrelated photons, 1, for different different frequencies, is scaling the original correlations.

### C. Dynamics of an out-of-equilibrium polariton condensate.

While we have dealt with the case of spontaneous emission exactly, it is clear that this is an awkward process. For the situation of our experiment, which corresponds instead to a steady state, we recourse to numerical calculations. Importantly, however, the two situations are not extremely different from a physical point of view. The emission indeed corresponds to spontaneous emission from a state whose coherence depends on the degree of condensation. The final phenomenology is extremely similar. We describe our system theoretically by the following minimal model which accounts for all the key ingredients of the experiments (Eq. (2) of the main text):

$$\frac{\partial \rho}{\partial t} = \left[ \frac{\gamma_a}{2} \mathcal{L}_a + \frac{\gamma_b}{2} \mathcal{L}_b + \frac{P_b}{2} \mathcal{L}_{b^\dagger} + \frac{P_{ba}}{2} \mathcal{L}_{a^\dagger b} \right] (\rho), \quad (\text{S37})$$

where  $\rho$  is the combined reservoir-condensate density matrix defined on the Hilbert space of two bosonic fields, since we describe both the BEC and the exciton reservoir by two harmonic modes  $a$  and  $b$ , which obey bosonic algebra  $[c, c^\dagger] = 1$ , with  $c = a, b$ . In the rotating frame of the frequency of the condensate, the dynamics is purely dissipative. Both modes lose particles, with decay rate  $\gamma_c$ , described by Lindblad terms:  $\sum_{O=a,b} \frac{\gamma_O}{2} \mathcal{L}_O(\rho)$ , where  $\mathcal{L}_O(\rho) = 2O\rho O^\dagger - O^\dagger O\rho - \rho O^\dagger O$ . The excitation is through the incoherent injection of reservoir excitons at a rate  $P_b$  with the accompanying Lindblad term  $\frac{P_b}{2} \mathcal{L}_{b^\dagger}(\rho)$ . The transfer of particles from the reservoir to the condensate, typically assumed to be phonon mediated, is described by the incoherent relaxation mechanism from  $a$  to  $b$ , described by a crossed Lindblad term  $\frac{P_{ba}}{2} \mathcal{L}_{a^\dagger b}(\rho)$ <sup>22</sup>. In an open system, such a reduced system is enough to capture the physics of condensation that otherwise requires a macroscopic reservoir with  $N$  states and  $N \rightarrow \infty$  to achieve coherence buildup<sup>37</sup>. This model has the minimum, but also all, ingredients to explain the core physical processes that takes place within our experimental conditions. It accounts successfully for, e.g., line narrowing and transition to lasing/condensation of the mode  $a$  when the pumping  $P_b$  is high enough, to all orders of the condensate field correlators  $N_{ab}[n, 0]$ , where:

$$N_{ab}[n, m] = \langle (a^\dagger)^n a^n (b^\dagger)^m b^m \rangle, \quad (\text{S38})$$

with  $n, m \in \mathbf{N}$  form a closed set under the dynamics of Eq. (S37)<sup>38</sup>. It is therefore also a sound model to compute theoretically the frequency-resolved correlations.

The zero-time delay dynamics is easily obtained:

$$\begin{aligned} \dot{N}_{ab}[n, m] = & - \left[ n\gamma_a + m(\gamma_b - P_b + P_{ba}) + nmP_{ba} \right] N_{ab}[n, m] \\ & + n^2 P_{ba} N_{ab}[n-1, m+1] + n P_{ba} N_{ab}[n, m+1] + P_b m^2 N_{ab}[n, m-1] - m P_{ba} N_{ab}[n+1, m]. \end{aligned} \quad (\text{S39})$$

Integrating these equations, it is possible to calculate, e.g., the condensate population,  $n_a = N_{ab}[1, 0]$ , the unnormalized second order correlation function at zero delay  $G^{(2)}(\tau=0) = N_{ab}[2, 0]$  or any other single time correlator. In particular, the steady state is obtained by setting  $\dot{N}_{ab}[n, m] = 0$  and solving the system of linear equations, which is finite when truncating to a large enough number of excitations. It is well known, and is straightforwardly shown, that  $g^{(2)}$  goes from values above 1, when  $P_b \ll \gamma_{b,a}$ , to 1 when  $P_b \gg \gamma_{b,a}$ , corresponding to a coherence buildup that accompanies condensation with  $n_a \gg 1$  and triggering a dynamics of relaxation dominated by stimulated emission<sup>37</sup>.

By following a similar procedure as in the previous section but for the case of a steady state<sup>18</sup> and the Liouvillian of Eq. (S37) we can compute (now numerically) the 2PS in this case. The result is shown in Fig. 2a of the main text and is indeed qualitatively very similar to the spontaneous emission case of a coherent state (where  $g^{(2)}(0) = 1$ ). In fact, the density plots may appear the same, but one can check by a more careful analysis that they are not exactly identical. The physics, however, has the same interpretation: a state with a given  $g^{(2)}(0)$  correlations emits photons which, if correlated in frequencies, exhibit an overall bunching when overlapping in time and frequencies and antibunching when overlapping in time but distinguished in frequencies.